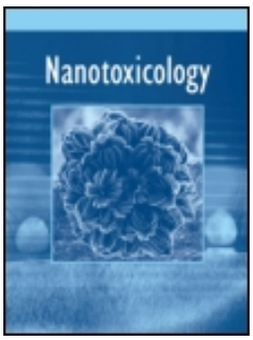

Nanotoxicology

ISSN: 1743-5390 (Print) 1743-5404 (Online) Journal homepage: https://www.tandfonline.com/loi/inan20

TiO_2 nanoparticles induce oxidative DNA damage and apoptosis in human liver cells

Ritesh K Shukla, Ashutosh Kumar, Deepak Gurbani, Alok K. Pandey, Shashi Singh & Alok Dhawan

To cite this article: Ritesh K Shukla, Ashutosh Kumar, Deepak Gurbani, Alok K. Pandey, Shashi Singh & Alok Dhawan (2013) TiO_2 nanoparticles induce oxidative DNA damage and apoptosis in human liver cells, Nanotoxicology, 7:1, 48-60, DOI: 10.3109/17435390.2011.629747

To link to this article: https://doi.org/10.3109/17435390.2011.629747

Published online: 02 Nov 2011.

Nanotoxicology, February 2013; 7(1):48–60

ISSN: 1743-5390 print / 1743-5404 online
DOI: 10.3109/17435390.2011.629747

informa
healthcare

ORIGINAL ARTICLE

TiO_2 nanoparticles induce oxidative DNA damage and apoptosis in human liver cells

Ritesh K. Shukla[1]*, Ashutosh Kumar[1]*, Deepak Gurbani[1], Alok K. Pandey[1], Shashi Singh[2], & Alok Dhawan[1]

[1]CSIR-Indian Institute of Toxicology Research, Nanomaterial Toxicology Group, Lucknow, Uttar Pradesh, India and [2]CSIR-Centre for Cellular and Molecular Biology, Council of Scientific and Industrial Research (CSIR), Hyderabad, Andhra Pradesh, India

Abstract

Titanium dioxide nanoparticles (TiO_2 NPs), widely used in consumer products, paints, pharmaceutical preparations and so on, have been shown to induce cytotoxicity, genotoxicity and carcinogenic responses *in vitro* and *in vivo*. The present study revealed that TiO_2 NPs induce significant ($p < 0.05$) oxidative DNA damage by the Fpg-Comet assay even at 1 μg/ml concentration. A corresponding increase in the micronucleus frequency was also observed. This could be attributed to the reduced glutathione levels with concomitant increase in lipid peroxidation and reactive oxygen species generation. Furthermore, immunoblot analysis revealed an increased expression of p53, BAX, Cyto-c, Apaf-1, caspase-9 and caspase-3 and decreased the level of Bcl-2 thereby indicating that apoptosis induced by TiO_2 NPs occurs via the caspase-dependent pathway. This study systematically shows that TiO_2 NPs induce DNA damage and cause apoptosis in HepG2 cells even at very low concentrations. Hence the use of such nanoparticles should be carefully monitored.

Keywords: Cellular uptake of TiO_2 NPs, oxidative stress; genotoxicity, HepG2, apoptosis

Introduction

Engineered nanoparticles (ENPs) are being widely used in electronics, engineering, therapeutics, diagnostic devices, pollutant remediation, personal care products and food/beverages. The increased use of ENPs has gained attention due to their adverse effects on the environment as well as on different animals and plants. The effects of ENPs depend on their size, shape, surface area, form and structure (Dhawan et al. 2009; Dhawan & Sharma 2010). TiO_2 has been classified as IARC-2B carcinogen (possibly carcinogenic to humans (IARC et al. 2006)). Titanium dioxide nanoparticles (TiO_2 NPs) are widely used in consumer products, paints, pharmaceutical preparations, food additives and so on and hence the likelihood of human exposure cannot be ignored. Toxicity assessment has shown that they can induce cytotoxic, genotoxic and carcinogenic responses both *in vitro* and *in vivo* (Johnston et al. 2009; Trouiller et al. 2009; Chen et al. 2010; Kim et al. 2010). Ultrafine TiO_2 have been shown to produce oxidative stress, DNA damage and inflammatory responses in human bronchial epithelial cells (BEAS-2B) without photo-activation (Gurr et al. 2005). TiO_2 NPs have also been reported to cause mutations and genotoxic responses in human lymphoblastoid cells (Wang et al. 2007b).

Previous studies have shown that interaction of free radicals (O_2^- production) with cellular components (nucleus, mitochondria, cytoplasm, etc.) results in the structural modification of cysteine, methionine, histidine, tryptophan and other amino acids (Hensley et al. 2000; Xia et al. 2009). Reactive oxygen species (ROS) attacks DNA and produces chain breaks, modification of carbohydrate parts and nitro bases by oxidation, nitration, methylation or deamination reactions, finally leading to cell death/apoptosis (Song et al. 2005). ROS also plays a key role in ENP-induced toxicity in cultured mammalian cells but limited data are available for the mechanism of toxicity.

The use of TiO_2 nanoparticles as food additive could result in these NPs reaching the non-target organs such as liver, spleen, lungs and so on. Bio-distribution of TiO_2 NPs leads to its accumulation in liver, causing hepatic injury (Wang et al. 2007a; Chen et al. 2009). TiO_2 NPs have been shown to induce oxidative stress and changes in the mitochondrial membrane potential at higher concentrations (100–250 μg/ml) in rat liver cell line (BRL 3A) (Hussain et al. 2005). Recently, it has also been shown that TiO_2 NPs (anatase and rutile) induce a genotoxic response as evidenced by up-regulation of p53 and down-regulation of DNA damage genes in human hepatocellular (HepG2) cells (Petkovic et al. 2011). However, the concentration of TiO_2 at which the study was undertaken

Correspondence: Professor Alok Dhawan, CSIR-Indian Institute of Toxicology Research, Nanomaterial Toxicology Group, Mahatma Gandhi Marg, P.O. Box 80, Lucknow–226001, Uttar Pradesh, India. Tel: +91 522 2230749. Fax: +91 0522 2628227, 2611547. E-mail: dhawanalok@hotmail.com; E-mail: alokdhawan@iitr.res.in
*These authors contributed equally to the manuscript.

(Received 13 June 2011; accepted 22 September 2011)

produces white precipitates. Also in this study the sonication of the particles was carried out in complete culture media that leads to degradation of fetal bovine serum (FBS). It was therefore prudent to conduct a systematic study and investigate the mechanism of genotoxicity as well as to see whether the DNA damage leads to apoptosis.

Materials and methods

Chemicals

Titanium (IV) oxide nanopowder (99.7%, anatase, CAS No. 1317-70-0), neutral red dye, low-melting-point agarose, ethidium bromide (EtBr), triton X-100, ethyl methanesulfonate (EMS), cytochalasin B, 2, 7-dichlorofluorescein diacetate (DCFDA), cell lysis buffer, *tert*-butyl hydroperoxide (t-BOOH), camptothecin, protease inhibitor and propidium iodide were purchased from Sigma Chemical Co. Ltd. (St Louis, MO, USA). Enzyme formamidopyrimidine DNA glycosylase (Fpg) was obtained from Trevigen Inc. (Gaithersburg, MD, USA). Normal-melting agarose (NMA), ethylenediaminetetraacetic acid (EDTA) disodium salt and 3-(4, 5-dimethylthiazol-2-yl)-2, 5-diphenyl tetrazolium bromide (MTT) dye were purchased from Hi-media Pvt. Ltd. (Mumbai, India). Phosphate-buffered saline (Ca^{2+}, Mg^{2+} free; PBS), minimal essential medium (MEM), trypsin-EDTA, FBS, trypan blue, antibiotic and antimycotic solution (10,000 U/ml penicillin, 10 mg/ml streptomycin, 25 μg/ml amphotericin-B) and 5,5',6,6' tetra ethylbenzimidazolocarbocyanine iodide (JC-1) dye were purchased from Life Technologies (India) Pvt. Ltd., (New Delhi, India). Giemsa stain powder was purchased from British Drug Houses Ltd. (Poole, England). Annexin V-FITC Apoptosis Detection kit was obtained from BD Pharmingen (San Jose, CA, USA). All other chemicals were obtained locally and were of analytical reagent grade.

Size determination of TiO_2 NPs using Transmission Electron Microscopy

Transmission electron microscopy (TEM) analysis of TiO_2 NPs was performed by preparing suspension (20 μg/ml) in milli-Q and placed on carbon-coated copper grids by drop-coating. The suspension on the grids was allowed to dry and TEM measurements were performed at an accelerating voltage of 120 kV (FEI; Tecnai G^2 F30 S-Twin, Oregon, USA).

Preparation of TiO_2 NPs suspension in culture media, characterisation and exposure to HepG2 cells

TiO_2 NPs (160 μg/ml) were suspended in IMEM (incomplete minimum essential medium; without FBS) and probe sonicated (Sonics Vibra cell, Sonics & Material Inc., New Town, CT, USA) for 10 min (1.5-min pulse on and 1-min pulse off for four times). After sonication, the suspension was diluted in CMEM (complete minimum essential medium; supplemented with 10% FBS) for cell exposure to ensure proper nutrition to the cells. The suspension sonicated did not contain FBS while the exposure media was supplemented with 10% FBS. The diluted TiO_2 NP concentrations in CMEM were then characterised by dynamic light scattering (DLS) instrument (Zetasizer Nano-ZS equipped with 4.0 mW, 633 nm laser (Model ZEN3600, Malvern instruments Ltd., Malvern, UK)). The size was also confirmed by TEM as reported in our earlier study (Shukla et al. 2011b). The human hepatocellular liver carcinoma cell line (HepG2) was obtained from National Centre for Cell Sciences, Pune, India, and cultured in MEM supplemented with 10% FBS, 0.2% sodium bicarbonate and 10 ml/L antibiotic and antimycotic solution at 37°C under a humidified atmosphere of 5% CO_2.

Stock suspension of TiO_2 NPs (160 μg/ml) in IMEM was diluted to concentrations ranging from 1 to 80 μg/ml (corresponding to 0.31–25 $\mu g/cm^2$) in CMEM respectively. HepG2 cells were exposed at varying concentrations for each experiment. Subsequent experiments involving cellular uptake assay, cytotoxicity assays, genotoxicity assays (Comet assay, micronucleus induction), oxidative stress marker (ROS generation, glutathione (GSH) depletion and lipid peroxidation (LPO)) and apoptosis markers (mitochondrial membrane potential assay, annexin-V and immunoblot assay) were conducted and analysed. For different assays, 96-, 12- and 6-well cell culture plates and 75 cm^2 cell culture flasks were used having a treatment volume of 0.1, 1.2, 3 and 24 ml respectively. However, the concentration per square centimetre area remained the same in all treatment regimes.

Cellular uptake of TiO_2 NPs

Flow cytometric detection of TiO_2 NPs was carried out according to the method of Suzuki et al. (2007) using light scattering principles.

TEM of TiO_2 NP-treated HepG2 cells

Ultrathin sections of cells were analysed using TEM to reveal the subcellular localisation of TiO_2 NPs in HepG2 cells. Similar protocol was used as described in our earlier study for A431 cells (Shukla et al. 2011b).

Cytotoxicity assays

Cytotoxicity assessment of TiO_2 NPs was determined by MTT and neutral red uptake (NRU) assay. These assays were carried out according to the method of Mosmann (1983) and Borenfreund & Puerner (1985), respectively, with slight modification as described in our earlier study (Shukla et al. 2011a, b). Briefly, 1×10^4 cells/well were seeded in 96-well plates and kept for 24 h. They were then exposed to different concentrations of TiO_2 NPs (0, 1, 10, 20, 40 and 80 μg/ml) for varying time intervals (6, 24 and 48 h). Nanoparticle interference with the assay reagents was also checked evenly using a cell free system. The results were assessed by measuring the absorbance of end product at their respective wavelengths using a SYNERGY-HT multiwell plate reader, Bio-Tek (USA) using KC4 software.

Genotoxicity assessment

The genotoxic potential of TiO_2 NPs was assessed by Fpg-modified Comet assay and cytokinesis-block micronucleus (CBMN) assay. The treatment scheme was same for both the assays. Approximately, 7×10^4 cells in 1.2 ml of MEM were seeded in a 12-well cell culture plate. After 24 h, the cells were exposed to TiO_2 NPs (1, 10, 20, 40 and 80 μg/ml) for 6 h. Hydrogen peroxide (25 μM) and ethyl methanesulfonate

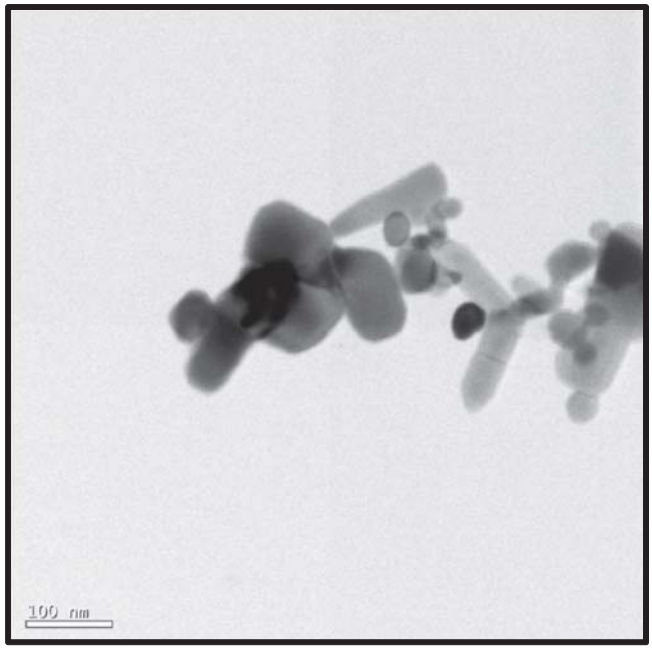

Figure 1. Transmission electron microscopy photomicrograph of titanium dioxide nanoparticles.

(6 mM) were used as positive control for Fpg-Comet assay and CBMN assay, respectively.

Fpg-Comet assay for detection of oxidative DNA damage

Cells were harvested and processed as given below:

The protocol involving lesion-specific DNA repair enzyme, formamidopyrimidine DNA glycosylase (Fpg) enzyme conjugated with Comet assay to identify the 8-oxoguanine and other damaged bases was performed according to Collins et al. (1996). Briefly, cells were harvested and slides were prepared by the method described by Singh et al. (1988) modified by Bajpayee et al. (2005). Slides were kept overnight at 4°C in lysis solution (2.5 M NaCl, 100 mM EDTA, 10 mM Tris (pH 10), 1% Triton X-100 added prior to lysis step). After lysis, slides were washed three times in enzyme buffer (40 mM HEPES, 0.1 M KCl and 0.5 mM EDTA, pH 8; 0.2 mg/mL BSA) and incubated with Fpg solution for 30 min at 37°C. Subsequently, alkaline unwinding of DNA was allowed for 20 min followed by electrophoresis in freshly prepared buffer (1 mM EDTA sodium salt and 300 mM NaOH) at 0.7 V/cm and 300 mA at 4°C for 30 min. Neutralisation was done using Tris buffer (400 mM, pH 7.4) and slides were stained with 20 μg/ml ethidium bromide (EtBr) and stored at 4°C in a humidified slide box until scoring.

Table I. Characterization of titanium dioxide nanoparticles using dynamic light scattering.

S. No	Dispersant	Hydrodynamic size (d.nm)	Polydispersity index (PDI)	Zeta potential (mV)
1.	Culture medium (CMEM)	192.5 ± 2.00	0.18 ± 0.01	-11.4 ± 0.25
2.	Milli Q	124.9 ± 3.20	0.12 ± 0.01	-17.6 ± 0.48

Values represent mean ± standard error of three experiments; CMEM, Complete minimum essential medium.

Scoring was done at a final magnification of 400× using Komet 5.0 software provided with the image analysis system (Andor Technology, Belfast, U.K.) attached with fluorescent microscope (DMLB, Leica, Wetzlar, Germany). The Comet parameters measured were tail DNA (%) and Olive tail moment (OTM). Analysis of 50 comets (25 from replicate slide) was carried out for each experiment according to Tice et al. (2000).

Cytokinesis-block micronucleus (CBMN) assay CBMN assay was carried out according to the method of Fenech (2000). After 6 h of exposure, the treatment of TiO_2 NPs was aspirated, washed with PBS and grown further for 20 h in complete medium containing cytochalasin-B at final concentration 3 μg/ml in 5% CO_2 incubator. The cells were harvested and slides were prepared by centrifugation using a cytospin (Thermo Shandon, Hampshire, UK). Two slides (two dots on one slide from each replicate culture) were prepared for each concentration. The slides were fixed in chilled methanol (90%) for 5 min, air-dried and stored until staining. The slides were stained with 10% Giemsa dissolved in Sorenson's buffer and examined for the presence of micronuclei in binucleate cells using light microscope (DMLB, Leica, Wetzlar, Germany) at 1000× magnification. Two thousand binucleate cells from each concentration (1000 binucleate cells from each slide, 500 cells per dot) were scored.

Oxidative stress markers

Cells at a final density of ~6×10^6 in a 75 cm^2 culture flask were exposed to different concentrations of TiO_2 NPs (1, 10, 20, 40, 80 μg/ml) for 6 h. t-BOOH (200 μM) was used as a positive control in GSH, LPO and ROS generation assays. After harvesting they were washed twice with chilled PBS, centrifuged at 500× g with pellet re-suspended in PBS and sonicated. Protein content was measured by Bradford's method (Bradford 1976).

GSH estimation

Treated cell lysate was used for estimation of total GSH content and expressed as micro moles/mg protein as described by Ellman (1959).

LPO assay

The LPO levels were estimated according to the manufacturer's protocol (Cayman Chemical Company, MI, USA). Briefly, lipid hydroperoxides were extracted from cell lysate into chloroform and solution containing ferrous ions was then added to cell extract, which on reaction with lipid hydroperoxide formed ferric ions. After 10 min, absorbance was measured at 500 nm.

Measurement of intracellular ROS

Intracellular ROS generation was estimated by the method of Wan et al. (1993) modified by Shukla et al. (2011b) using DCFDA dye. The interference and autofluorescence of TiO_2 NPs with DCFDA was also monitored in a parallel experiment without cells. The % ROS generation was calculated using the following formula, after correcting for background fluorescence:

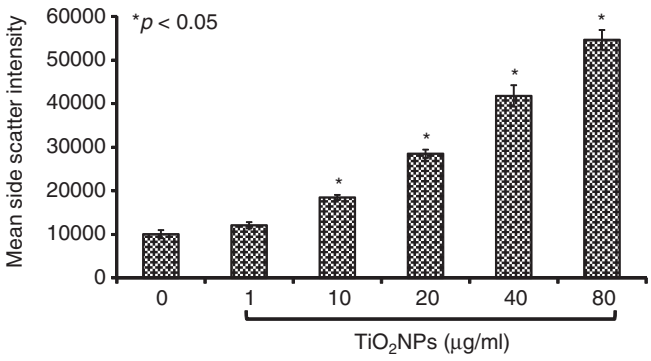

Figure 2. Analysis of internalisation of nanoparticles by flow cytometric parameter viz. side scatter intensity. HepG2 cells exposed to titanium dioxide (TiO_2) NPs (0–80 µg/ml) for 6 h. Results expressed as mean ± SE from three independent experiments ($^*p < 0.05$).

$$\%\ \text{ROS generation} = [(F\ 485/528_{\text{sample}} - F\ 485/528_{\text{sample blank}})/(F\ 485/528_{\text{control}} - F\ 485/528_{\text{control blank}})] \times 100$$

Apoptosis Markers

Mitochondrial membrane potential

Mitochondrial membrane potential ($\Delta\psi$) was measured using lipophilic cationic dye JC-1, which selectively enters mitochondria and changes its colour reversibly from red to green if membrane potential decreases. Cells undergoing apoptosis were detected using a flow cytometer at excitation/emission wavelengths 488 nm/527 nm (Salvioli et al. 1997). Briefly, 2×10^5 cells/well were seeded in 6-well culture plate for 24 h prior to exposure to TiO_2 NPs. Cells were treated with TiO_2 NPs (0, 20, 40 and 80 µg/ml) for 24 h. Non-treated cells served as a negative control and camptothecin (1 µM) was used as positive control. After removal of treatment, cells were washed with PBS and incubated with 10 µM of JC-1 dye for 15 min at 37°C. The cells were analysed using BD FACSCanto II flow cytometer and software provided with the instrument (BD FACS Diva 6.2.1 software, BD Biosciences, San Jose, CA, USA).

Annexin V binding assay

Actively undergoing apoptotic cells were identified by staining with fluorescein isothiocyanate-conjugated (FITC)-annexin V and PI according to the manufacturer's protocol (BD Biosciences, San Jose, CA, USA). Briefly, 2×10^5 cells/well was seeded in a 6-well culture plate for 24 h prior to treatment. Cells were treated with TiO_2 NPs at

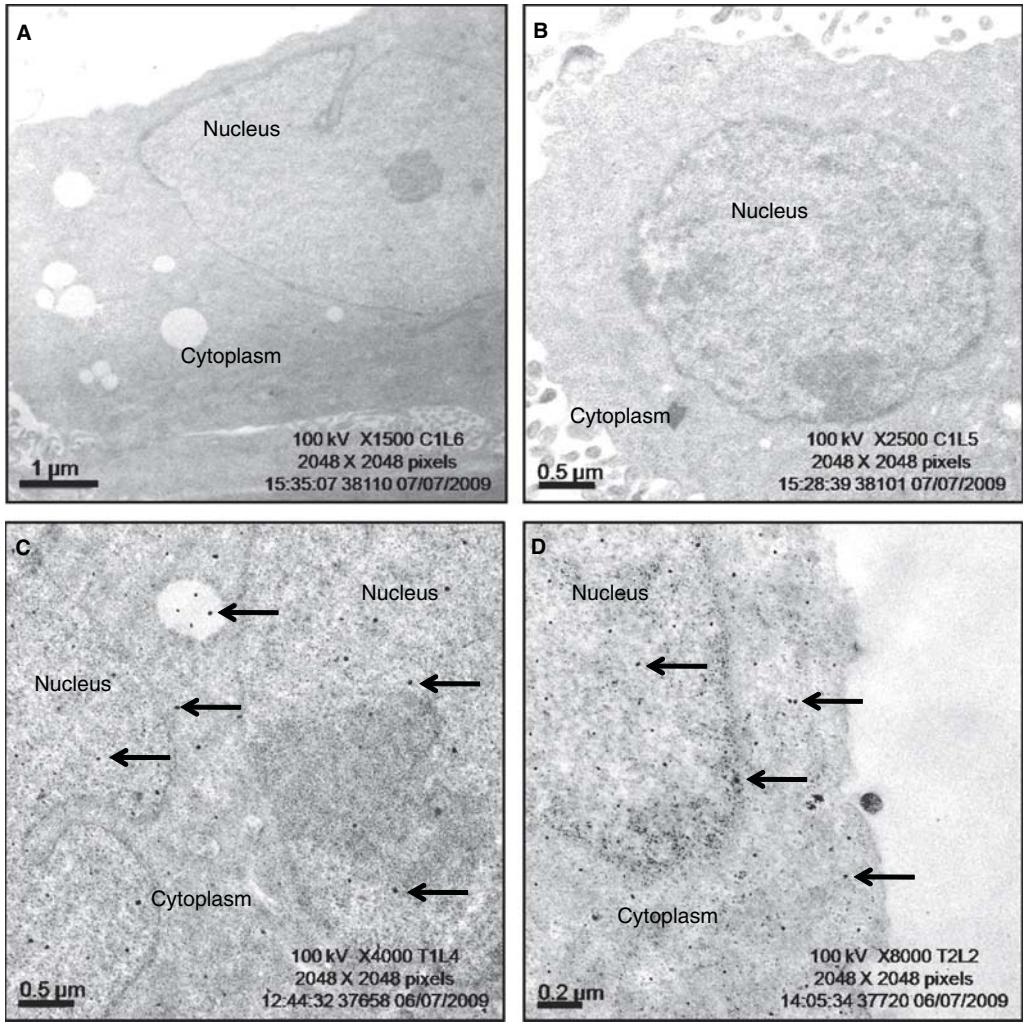

Figure 3. Electron photomicrographs of HepG2 cells showing internalisation of titanium dioxide nanoparticles (TiO_2 NPs) in (A–B) control, (C) cytoplasm and (D) nucleus. Arrows indicate the presence of TiO_2 NPs.

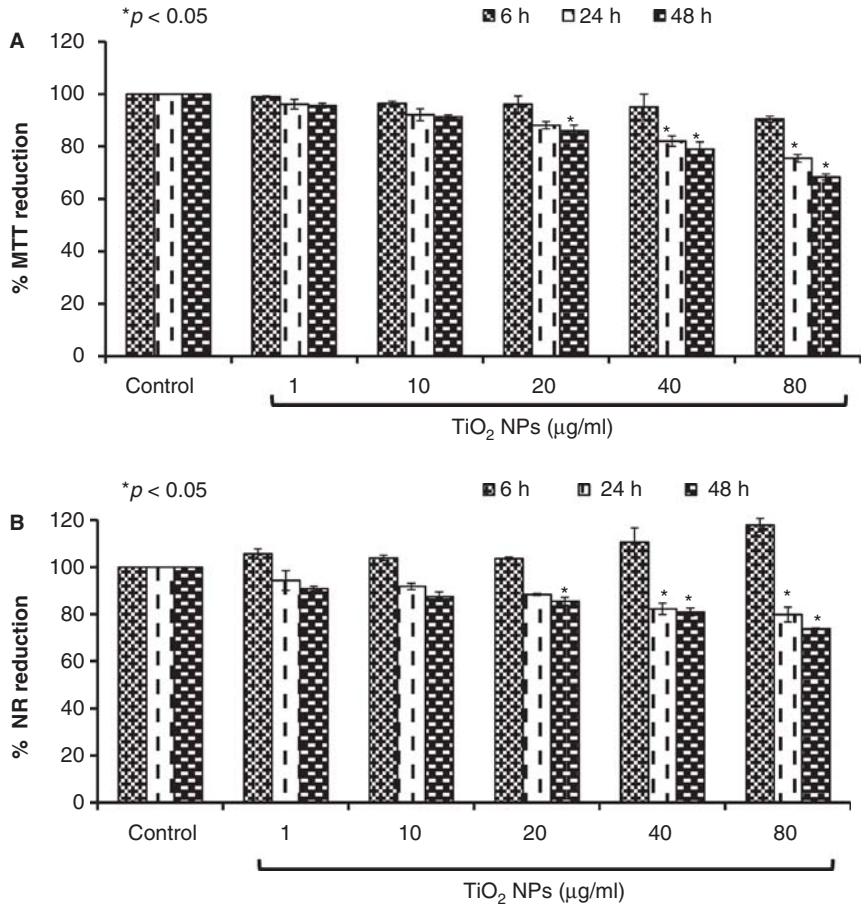

Figure 4. Concentration and time-dependent cytotoxicity of titanium dioxide nanoparticles (TiO_2 NPs) in HepG2 cells.(A) % MTT reduction, (B) % neutral red uptake. The viability of the control cells was considered as 100%. The data are expressed as mean ± SEM from three independent experiments. * $p < 0.05$, when compared with control.

different concentrations (0, 20, 40 and 80 µg/ml) for 48 h. In this assay, 1 µM camptothecin was used as a positive control. After removal of treatment, cells were harvested and washed twice with PBS, re-suspended in 0.1 ml binding buffer containing 5 µl of FITC-annexin V and PI and kept at room temperature in dark. After 10 min of incubation, 0.4 ml of binding buffer was further added to each sample and analysed using flow cytometer.

Immunoblot analysis

HepG2 cells were treated with TiO_2 NPs at concentrations 20, 40 and 80 µg/ml for 48 h. After treatment removal, cells were harvested and lysed in lysis buffer (150 mM NaCl, 1% NP-40, 1% sodium deoxycholate, 0.1% SDS, 50 mM Tris–HCl, pH 7.5, 2 mM EDTA) containing protease inhibitor cocktail (Sigma, USA). Protein concentration was estimated using Bradford's method (Bradford 1976). Protein (50 µg) from control and treated groups was separated on tricine-SDS-polyacrylamide gel (12%) and transferred to a nitrocellulose membrane by electroblotting. The membrane was incubated with primary antibodies specific for p53, Bax, Bcl-2, hsp60, 70, caspase-3, -9, Apaf-1 and cytochrome c and β-actin (Millipore, India). Secondary antibody incubation was done and protein bands were detected using chemiluminescence and densitometric analysis was carried out using Quantity One Quantitation Software© version 4.3.1 (Bio-Rad, USA).

Table II. DNA damage in HepG2 cells after 6 h exposure to titanium dioxide nanoparticles (TiO_2 NPs) as evident by the Comet parameters.

Groups	OTM (arbitrary unit)		Tail DNA (%)	
	Fpg (-)	Fpg (+)	Fpg (-)	Fpg (+)
Control (0 µg/ml)	0.94 ± 0.06	0.96 ± 0.04	7.75 ± 0.36	7.85 ± 0.52
Positive control – H_2O_2 (25 µM)	3.14 ± 0.26*	5.04 ± 0.18*α	21.04 ± 1.36*	27.13 ± 1.18*α
TiO_2 NPs (1 µg/ml)	1.13 ± 0.06	1.35 ± 0.13*α	8.61 ± 0.67	9.54 ± 0.72
TiO_2 NPs (10 µg/ml)	1.20 ± 0.05*	1.58 ± 0.08*α	9.13 ± 0.54	11.36 ± 0.50*α
TiO_2 NPs (20 µg/ml)	1.40 ± 0.02*	1.95 ± 0.17*α	10.53 ± 0.49*	14.16 ± 0.14*α
TiO_2 NPs (40 µg/ml)	1.55 ± 0.07*	2.18 ± 0.10*α	11.61 ± 0.38*	16.12 ± 0.26*α
TiO_2 NPs (80 µg/ml)	1.76 ± 0.09*	2.81 ± 0.12*α	13.55 ± 0.43*	20.86 ± 1.45*α

Values represent mean ± S.E. of three experiments; *$p < 0.05$ when compared with control using one-way ANOVA; $^{\alpha}p < 0.05$ using when compared with Fpg (-) at the same concentration using Student 't' test; OTM, Olive tail moment.

Table III. Effect of titanium dioxide nanoparticles (TiO_2 NPs) on micronucleus formation in HepG2 cells.

Groups	No. of MN/1000 binucleated cells
Control (0 μg/ml)	7.00 ± 0.58
EMS[a]	23.33 ± 1.45***
TiO_2 NPs (1 μg/ml)	8.00 ± 1.15
TiO_2 NPs (10 μg/ml)	11.00 ± 1.53*
TiO_2 NPs (20 μg/ml)	15.00 ± 0.58**
TiO_2 NPs (40 μg/ml)	12.33 ± 0.33**
TiO_2 NPs (80 μg/ml)	10.67 ± 0.88*

Values represent mean ± S.E. of three experiments for each concentration; [a]EMS – ethyl methanesulfonate-positive control (6 mM); *$p < 0.05$; **$p < 0.01$; ***$p < 0.001$ when compared with control.

Statistical analysis

Results from each experiment were expressed as mean ± SEM of three individual experiments and data were analysed using one-way analysis of variance (ANOVA). The post hoc comparisons of mean of independent groups were done by Dunnett's test at statistically significant values ($p < 0.05$).

Results

The study revealed the uptake and cellular internalisation of TiO_2 NPs in HepG2 cells. These particles upon internalisation produced genotoxic effects, oxidative DNA damage and disruption of mitochondrial membrane, thereby leading to apoptosis. The detail results are described below:

Measurement of TiO_2 nanoparticles

The size of TiO_2 NPs as revealed by TEM ranged between 30 to 70 nm (Figure 1). DLS measurements showed a mean hydrodynamic diameter of TiO_2 NPs in Milli Q and culture media to be 124.9 and 192.5 nm respectively (Table I). However, the zeta potential changed from -17.6 mV in Milli Q to -11.4 mV in culture media (MEM supplemented with 10% FBS).

Cellular uptake of TiO_2 NPs

Flow cytometric analysis revealed a significant ($p < 0.05$) concentration-dependent increase in the cellular internalisation of TiO_2 NPs after 6 h exposure (Figure 2). This was evident by increase in the side scatter intensity (granularity) of TiO_2 NP-treated cells in a concentration-dependent manner. Furthermore, subcellular localisation of TiO_2 NPs inside cytoplasm and nucleus was confirmed using TEM (Figure 3).

Evaluation of TiO_2 NP-induced cytotoxicity

Cytotoxicity of TiO_2 NPs was assessed for 6, 24 and 48 h respectively. In the MTT assay, mitochondrial succinate dehydrogenase activity in HepG2 cells was reduced to 82% and 75% (relative to 100% of control) at 40 and 80 μg/ml after 24 h exposure, which further reduced up to 79% and 68% respectively after 48h exposure (Figure 4A). NRU uptake assay showed that NRU was reduced to 82% and 81% at 40 μg/ml treatment of TiO_2 NPs whereas it further reduced to 79% and 73% at 80 μg/ml at 24 and 48 h exposure when compared with control (Figure 4B). However, no significant cytotoxic effect of TiO_2 NPs was observed at 6 h exposure in both the assays.

Genotoxic potential of TiO_2 NPs

Oxidative DNA damage using Fpg-Comet assay

The Fpg-modified Comet assay revealed a significant ($p < 0.05$) concentration-dependent increase in oxidative DNA damage in response to TiO_2 NP exposure as analysed using qualitative and quantitative parameters of the Comet assay viz. OTM and % Tail DNA respectively (Table II). A statistically significant ($p < 0.05$) induction in DNA damage was observed at the different concentration of TiO_2 NPs (10–80 μg/ml) after 6 h exposure as compared with the respective

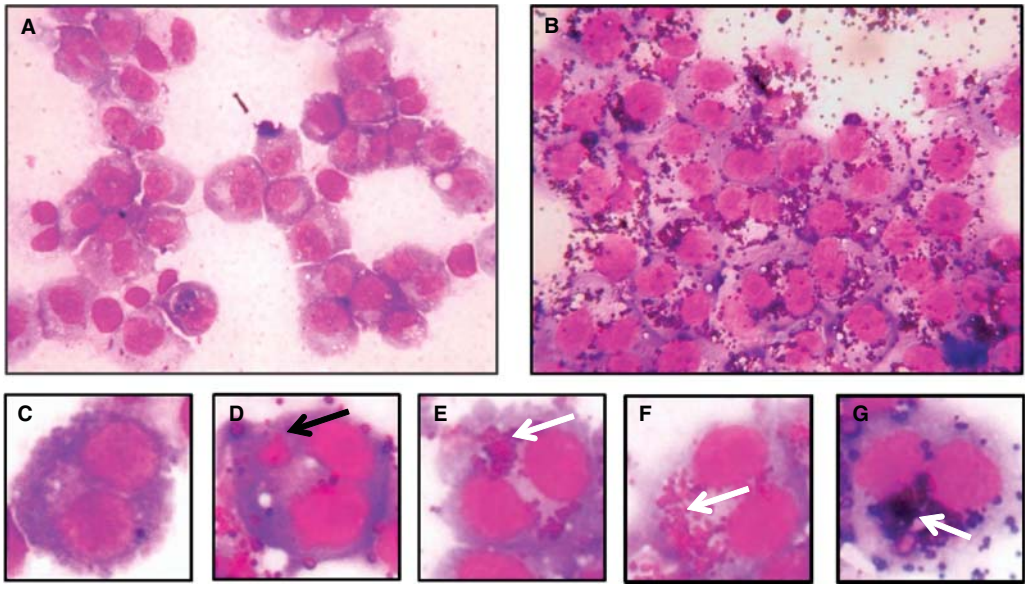

Figure 5. Photomicrographs of HepG2 Cells showing CBMN assay. (A) Field view of control cells, (B) field view of titanium dioxide nanoparticle (TiO_2 NP)-exposed cells. Magnification X400. (C) Control binucleate cell, (D) TiO_2 NP-exposed binucleate cell showing micronucleus indicated by black arrow. (E–F) TiO_2 NP-exposed binucleate cells showing presence of nanoparticles at the position of micronucleus indicated by white arrow.

control cells in standard Comet assay. However, TiO_2 NPs induced significant oxidative DNA damage even at 1 μg/ml concentration as evident by the Fpg treatment (Table II). When compared among the groups, Fpg elicited a significantly greater response at all the concentrations of TiO_2 NPs (1, 10, 20, 40 and 80 μg/ml) as evident by the Comet assay parameter.

Micronucleus induction

TiO_2 NPs induced a statistically significant ($p < 0.05$) increase in the number of micronucleated cells at 20 μg/ml (15.00 MN/1000 BNCs) when compared with the control (7.00 MN/1000 BNCs) after 6 h exposure. However, on further increasing the concentrations (40 and 80 μg/ml), the micronucleus formation decreased (Table III). A large number of TiO_2 NPs were also seen at these concentrations (Figure 5).

Evaluation of Oxidative stress

TiO_2 NPs caused a significant ($p < 0.05$) concentration-dependent increase in intracellular ROS (77.78%, 114.83%, 131.59% and 143.65% at concentrations of 10, 20, 40 and 80 μg/ml respectively) as evident by an increase in the fluorescence intensity of DCFDA dye (Figure 6A).

A similar effect was observed on the antioxidant defence system where significant ($p < 0.05$) decrease in intracellular GSH levels (19.39%, 25.07% and 29.51%) of HepG2 cells was observed (20, 40 and 80 μg/ml) at 6 h exposure of TiO_2 NPs (Figure 6B). TiO_2 NPs also caused LPO, as a concentration-dependent statistically significant ($p < 0.05$) increase in hydroperoxide concentration was observed at 20 (54.06%), 40 (59.05%) and 80 μg/ml (87.35%; Figure6C).

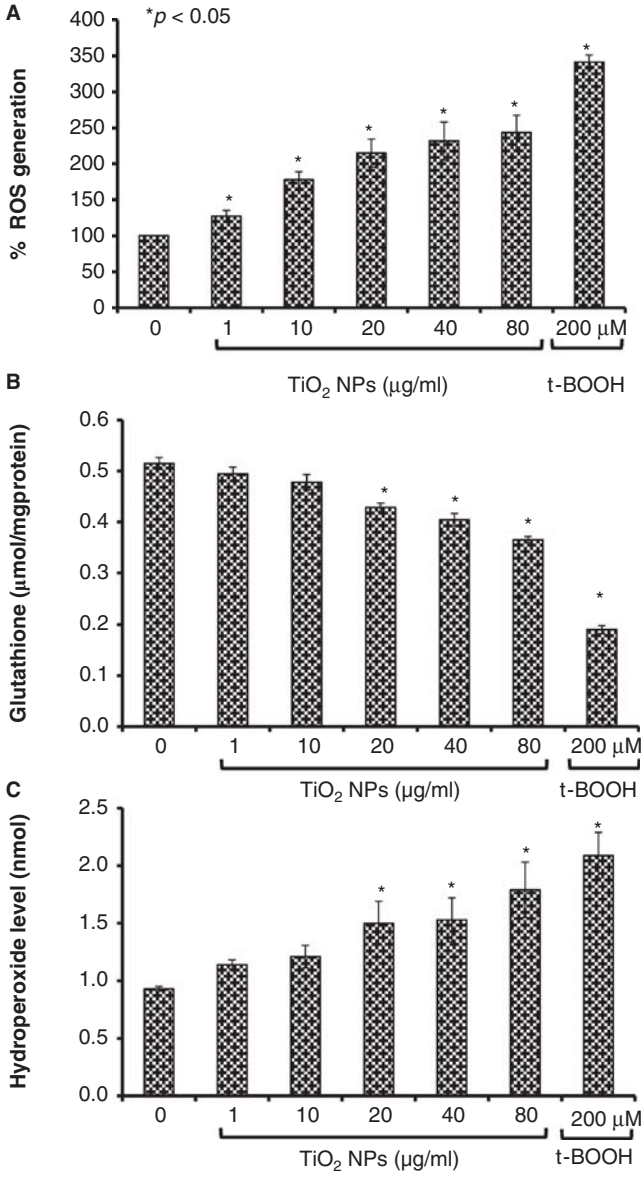

Figure 6. Effects of titanium dioxide nanoparticles (TiO_2 NPs) on (A) reactive oxygen species (ROS), (B) glutathione (GSH) and (C) lipid peroxidation (LPO) levels in HepG2 cells. t- BOOH (200 μM) was used as positive control. Data represent mean ± SEM from three independent experiments.*$p < 0.05$, when compared with control.

Extent and mode of Apoptosis

HepG2 cells treated with TiO_2 NPs (0, 20, 40 and 80 μg/ml) for 24 h demonstrated alteration in the mitochondrial membrane integrity as evidenced by JC-1 dye analysed using flow cytometry (Figure 7A). A significant ($p < 0.05$) increase in the green fluorescence intensity (7.6 ± 0.21%, 14.8 ± 1.4% and 16.9 ± 0.82%) was observed when compared with control (4.8 ± 0.27%; Figure 7A–B). Furthermore, early and late apoptotic cells were detected using annexin V-PI dual staining assay. The data revealed the presence of apoptotic and necrotic cells upon TiO_2 NPs exposure at concentrations of 20, 40 and 80 μg/ml after a 48 h exposure. Early apoptotic cells increased from 4.2% (control) to 14.5% (20 μg/ml), 22.6% (40 μg/ml) and 21.7% (80 μg/ml) whereas late apoptotic cells increased from 1.5% (control) to 8.9% (20 μg/ml), 8.9% (40 μg/ml) and 10% (80 μg/ml). Similarly, necrosis was also observed in a dose-dependent manner with maximum (11%) at 80 μg/ml (Figure 8A–B). To evaluate the mode of action of apoptosis by TiO_2 NPs, induction of key apoptotic marker proteins was examined. Immunoblot analysis of HepG2 cells treated with TiO_2 NPs (40 and 80 μg/ml) for 6 h exposure showed significant increase ($p < 0.05$) in the expression of stress proteins hsp60 (54%, 80%), hsp70 (30%, 62%; Figure 9A) and for 48 h exposure showed significant increase in the expression of tumour suppressor protein p53 (43%, 60%), cytochrome c (35%, 52%), Bax (18%, 24%), caspase-9 (37%, 49%), caspase-3 (21%, 29%), Apaf-1 (22%, 34%) with decreased expression of anti-apoptotic mitochondrial protein Bcl-2 (28%, 37%) as shown in Figure 9B and Figure 9C.

Discussion

The present study has systematically examined the effects of TiO_2 NPs in human liver cells (HepG2 cells). It has been shown that TiO_2 NPs induce oxidative DNA damage and apoptosis in HepG2 cells through mitochondria-mediated pathway.

Characterisation of NPs is essential due to the fact that shape, size, surface area, surface charge, monodispersity and

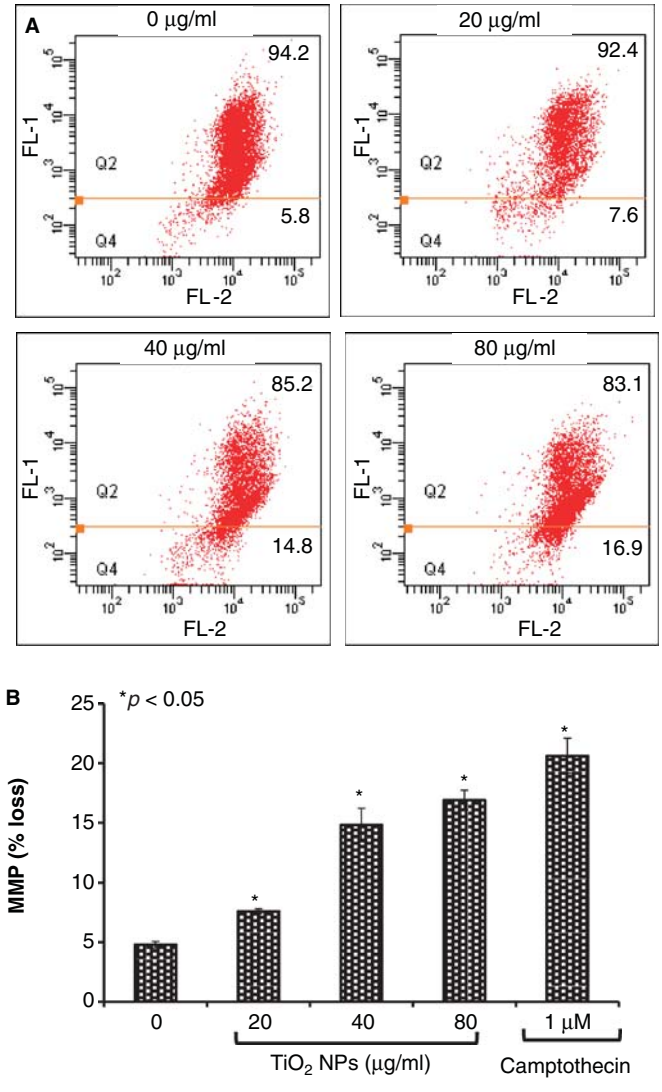

Figure 7. Titanium dioxide nanoparticle (TiO_2 NP)-induced loss of mitochondrial membrane potential (MMP) in HepG2 cells. (A) Distribution of JC-1 aggregates and monomers after 24 h exposure and (B) bar graph shows the percentage of JC-1 monomer positive cells (%MMP loss). Camptothecin (1 μM) was used as positive control. Data of % MMP loss are expressed as mean ± SEM from three independent experiments.* $p < 0.05$, when compared with control.

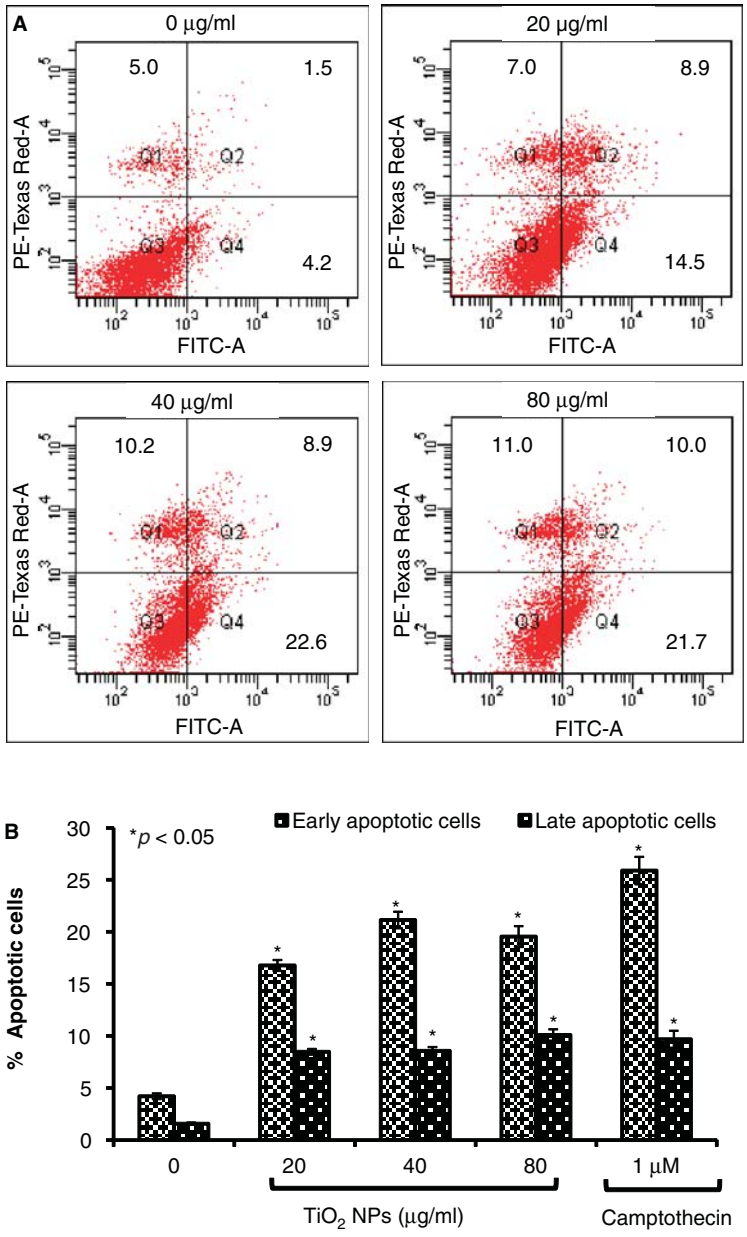

Figure 8. Evaluation of early and late apoptotic cells by the annexin-V staining. (A) Four subpopulations and their percent distribution in different quadrants: necrotic cells (Q1), late apoptotic cells (Q2), viable cells (Q3) and early apoptotic cells (Q4). (B) Bar graph showing per cent apoptotic cells. Camptothecin (1 µM) was used as positive control. Data represent mean ± SEM of three independent experiments.*$p < 0.05$, when compared with control. FITC-A, fluorescein isothiocyanate-conjugated annexin V; TiO_2 NPs, titanium dioxide nanoparticles.

so on affect physiochemical properties responsible for differential responses observed within biological systems (Dhawan et al. 2009). Studies so far have used a variety of methods for size determination of nanoparticles in dry powder form using TEM and in liquid suspension or culture media using DLS respectively (Sharma et al. 2009; Kumar et al. 2011; Sharma et al. 2011). Our TEM measurements and DLS analysis showed that TiO_2 NPs were stable and monodispersed in culture media, making them suitable for toxicity studies.

Since these NPs have smaller distribution size range, they can easily enter and localise inside cells. The present study through TEM measurements demonstrates that TiO_2 NPs get internalised into the cell and localise in the cytoplasm as well as the nucleus. This could help in explaining the oxidative stress and DNA damage observed. These findings were also consistent with our flow cytometry analysis where concentration-dependent increase in the intensity of side scatter (due to particle uptake) was observed. Similar studies have been carried out using Chinese hamster ovary and primary culture cells (Suzuki et al. 2007; Xu et al. 2009). Distribution of these TiO_2 NPs inside cells would therefore enable interactions with biological macromolecules, including lipids, proteins and nucleic acids thereby eliciting toxic responses.

Studies so far have focused on cytotoxic, genotoxic effects mediated by oxidative stress. Recently, it has been reported in HepG2 cells (Petkovic et al. 2011) that exposure to TiO_2 NPs at 250 µg/ml concentration leads to two-fold increase in ROS levels at 5 h exposure duration thereby causing DNA

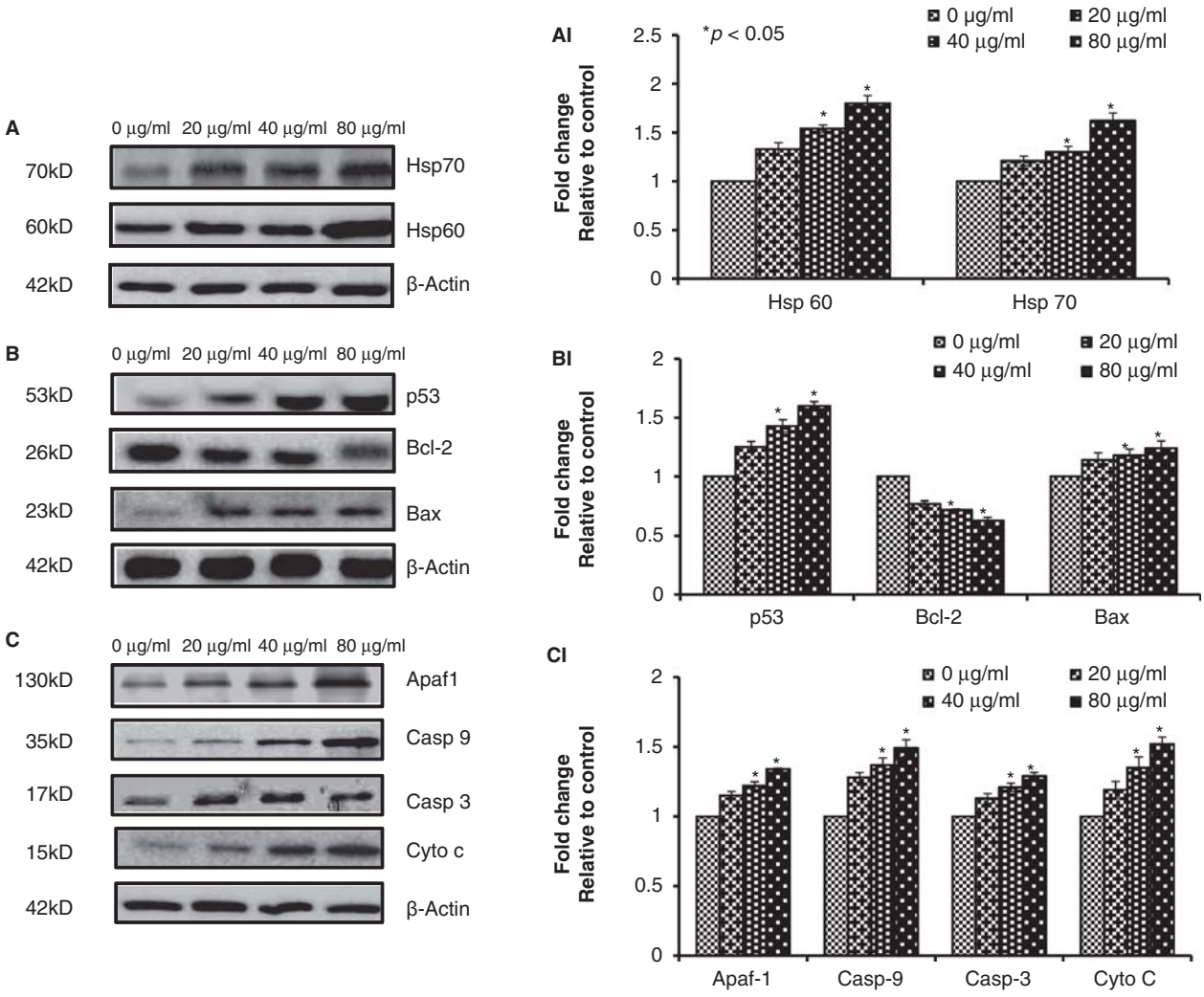

Figure 9. Immunoblot analysis of proteins of HepG2 cells treated with different concentrations (20, 40 and 80 µg/ml) of titanium dioxide nanoparticles. β-actin was used as an internal control. (A) Stress proteins (Hsp60, Hsp70; 6-h exposure); (B–C) apoptotic proteins (p53, Bax, Bcl-2; Apaf-1, caspase-9, caspase-3, cyto c, 48 h exposure) and the corresponding (A1, B1 and C1) bar graphs exhibiting their densitometric analysis.

damage. Since no data on the stability of the particles were provided, it is difficult to interpret the results from such a study using high concentrations. Our earlier studies with TiO_2 (Anatase) from the same company (Sigma-Aldrich) have shown that the particles tend to agglomerate and even precipitate at concentrations above 80 µg/ml in the absence of a stabiliser such as propylene glycol (Gurbani et al. 2011).

In the present study, we used a range of TiO_2 NP concentrations (1, 10, 20, 40 and 80 µg/ml) for different time points (6, 24 and 48 h). Initially the cytotoxicity experiments were performed for all the concentrations and time points. The cells were more than 90% viable after 6 h exposure of TiO_2 ENPs. Hence, these non-cytotoxic concentrations and time points were used for genotoxicity studies and their mechanistic studies (oxidative stress).

However, our data also exhibit that only at 20, 40 and 80 µg/ml TiO_2 NP concentrations, a significant cytotoxicity was observed after 24 and 48 h exposure. Hence, these concentrations were further used for mitochondrial membrane potential and annexin V binding assay to demonstrate apoptosis. Our data exhibited a significant MMP loss after 24 h exposure; however, the annexin V binding was not significant. Hence the annexin V binding assay and immunoblot analysis were performed after 48 h exposure at concentrations 20, 40 and 80 µg/ml.

Our study showed that TiO_2 NPs induce stress in HepG2 cells as evident by an induction of Hsp60 and Hsp70. Hsp family of proteins is the first tier of cellular defence that induces the protein folding to minimise degradation and cellular stress. Furthermore, greater than two-fold induction in ROS generation and depletion in GSH levels with a concomitant increase in LPO revealed that TiO_2 NPs induce oxidative stress. Our findings are in accordance with the previous studies in different cell types where TiO_2 has been shown to produce ROS even without photoactivation (Park et al. 2008; Shukla et al. 2011a, b).

Further oxidative DNA damage was observed in the HepG2 cells after treatment with TiO_2 NPs. This could be due to the ROS generation even at lower concentration of 1 µg/ml of TiO_2 NPs. 8-Hydroxy-deoxyguanosine (8-OHdG) is the major oxidative DNA damage product that can produce

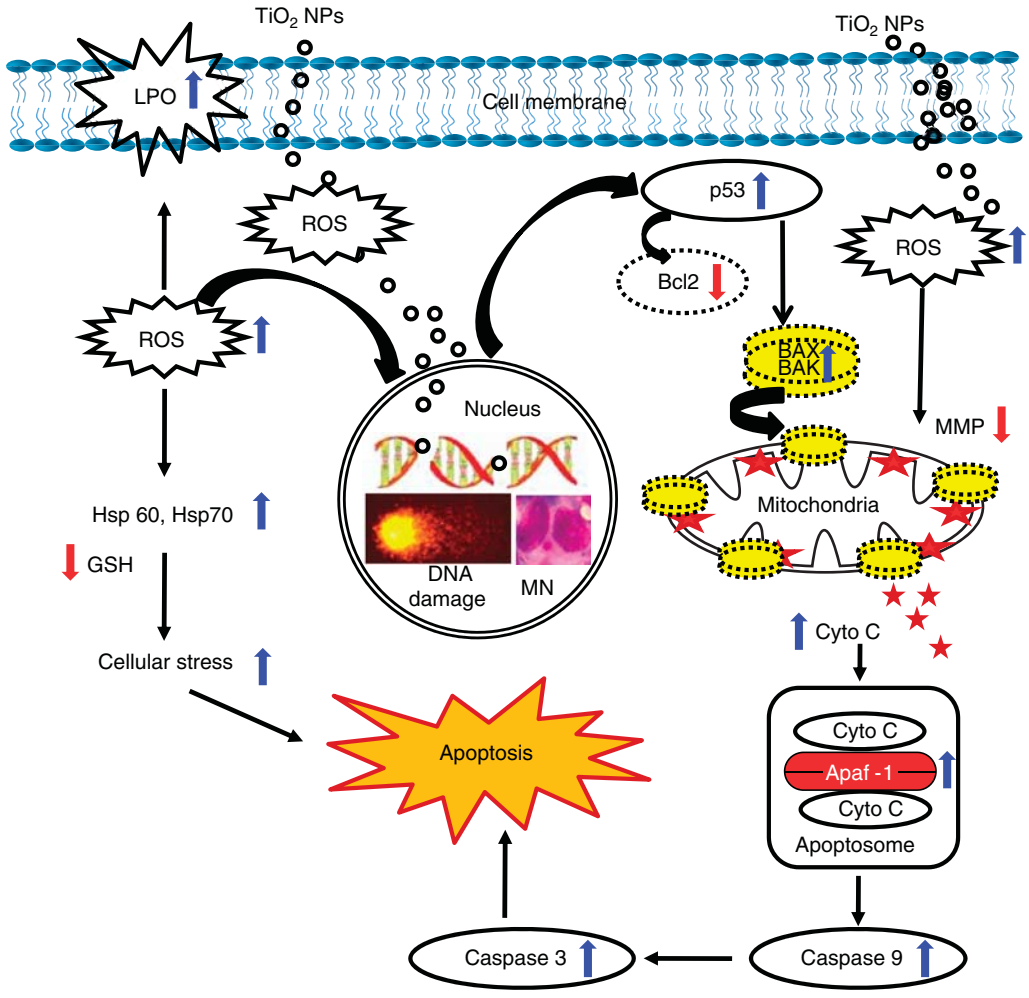

Figure 10. A schematic showing possible mechanisms of titanium dioxide nanoparticles (TiO_2 NPs)-induced cellular toxicity in HepG2 cells.

mutations – A: T to G: C or G: C to T: A transversion mutations – since it base pairs with adenine as well as cytosine (Valko et al. 2004). The data from Fpg-Comet strengthened our assumption that TiO_2 NPs induces ROS-mediated oxidative DNA damage. Furthermore, TiO_2 NPs significantly induced ($p < 0.05$) micronucleus formation in a concentration-dependent manner. At higher concentrations (40 and 80 µg/ml), the micronucleus formation was slightly less than that observed at 20 µg/ml. This may be due to the deposition of TiO_2 NPs on the slides during the slide preparation, which hinders the counting of micronucleus as observed in our study as well as by others (Figure 5; Falck et al. 2009; Di Virgilio et al. 2010).

The present study also investigated the induction of apoptosis by TiO_2 NPs in HepG2 cells. Our data revealed the presence of early apoptotic cells as evident by a decrease in the mitochondrial membrane potential at 24 h. TiO_2 NPs have also been shown to induce oxidative stress leading to apoptosis in cultured human lung epithelial cells (BEAS-2B cells), rat neuronal cells (PC-12) and mouse epidermal cells (JB-6) (Park et al. 2008; Zhao et al. 2009; Hussain et al. 2010; Liu et al. 2010).

However at 48 h, cells undergoing late apoptosis and necrosis were observed by annexin V/PI assay. To decipher the mechanism behind mitochondria-mediated apoptosis, p53 levels were measured in HepG2 cells after exposure to TiO_2 NPs. The immunoblot analysis showed a concentration-dependent increase in the expression of p53. Our data exhibited a concentration-dependent increase in the expression of BAX (pro-apoptotic) and decrease in levels of Bcl-2 (anti-apoptotic). This could be due to increased p53 levels, which result in the modulation in the Bax/Bcl-2 ratio. This leads to the release of cytochrome c, which binds to the apoptotic protease-activating factor (Apaf-1) resulting in the formation of an apoptosome. Our data also suggest that caspase-9 and caspase-3 activation lead to cascade of events that trigger cell death in TiO_2 NP-treated HepG2 cells. A pathway for TiO_2 NP-induced apoptosis in HepG2 cells is depicted in Figure 10.

The present study systematically demonstrates the role of mitochondrial intrinsic pathway for TiO_2 NP-induced apoptosis in HepG2 cells, which could be attributed to ROS-mediated DNA damage.

Acknowledgment

The authors gratefully acknowledge the funding from CSIR, New Delhi, under its network project (NWP35),

Supra institutional Project (SIP-008), OLP 009. The funding from the Department of Science and Technology, Government of India, under the nano mission project – DST-NSTI grant (SR/S5/NM-01/2007) and UK India Education and Research Initiative (UKIERI) standard award to Indian Institute of Toxicology Research, Lucknow, India (DST/INT/UKIERI/SA/P-10/2008), and the Department of Biotechnology, under the New INDIGO programme (NanoLINEN project) is gratefully acknowledged. RKS thanks University Grant Commission (UGC), New Delhi, for the award of Senior Research Fellowship. AK gratefully acknowledges ICMR-SRF fellowship.

Declaration of interest

The authors report no conflicts of interest. The authors alone are responsible for the content and writing of the paper.

References

Bajpayee M, Pandey AK, Parmar D, Mathur N, Seth PK, Dhawan A. 2005. Comet assay responses in human lymphocytes are not influenced by the menstrual cycle: a study in healthy Indian females. Mutat Res 565:163–172.

Borenfreund E, Puerner JA. 1985. Toxicity determined in vitro by morphological alterations and neutral red absorption. Toxicol lett 24:119–124.

Bradford MM. 1976. A rapid and sensitive method for the quantitation of microgram quantities of protein utilizing the principle of protein-dye binding. Anal Biochem 72:248–254.

Chen J, Dong X, Zhao J, Tang G. 2009. In vivo acute toxicity of titanium dioxide nanoparticles to mice after intraperitioneal injection. J Appl Toxicol 29:330–337.

Chen J, Zhou H, Santulli AC, Wong SS. 2010. Evaluating cytotoxicity and cellular uptake from the presence of variously processed TiO2 nanostructured morphologies. Chem Res Toxicol 23:871–879.

Collins A, Dusinska M, Gedik C, Stetina R. 1996. Oxidative damage to DNA: do we have a reliable biomarker? Environ Health Perspect 104:465–469.

Dhawan A, Sharma V, Parmar D. 2009. Nanomaterials: a challenge for toxicologists. Nanotoxicology 3:1–9.

Dhawan A, Sharma V. 2010. Toxicity assessment of nanomaterials: methods and challenges. Anal bioanal chem 398:589–605.

Di Virgilio AL, Reigosa M, Arnal PM, Fernandez M, Mele LD. 2010. Comparative study of the cytotoxic and genotoxic effects of titanium oxide and aluminium oxide nanoparticles in Chinese hamster ovary (CHO-K1) cells. J Hazard Mater 177:711–718.

Ellman GL. 1959. Tissue sulfhydryl groups. Arch Biochem Biophys 82:70–77.

Falck GC, Lindberg HK, Suhonen S, Vippola M, Vanhala E, Catalan J, et al. 2009. Genotoxic effects of nanosized and fine TiO2. Hum Exp Toxicol 28:339–352.

Fenech M. 2000. The in vitro micronucleus technique. Mutat Res 455:81–95.

Gurbani D, Shukla RK, Pandey AK, Dhawan A. 2011. Stable metal oxide nanoparticle formulation for toxicity studies. J Biomed Nanotechnol 7:104–105.

Gurr JR, Wang AS, Chen CH, Jan KY. 2005. Ultrafine titanium dioxide particles in the absence of photoactivation can induce oxidative damage to human bronchial epithelial cells. Toxicology 213:66–73.

Hensley K, Robinson KA, Gabbita SP, Salsman S, Floyd RA. 2000. Reactive oxygen species, cell signaling, and cell injury. Free Radic Biol Med 28:1456–1462.

Hussain S, Thomassen LC, Ferecatu I, Borot MC, Andreau K, Martens JA, et al. 2010. Carbon black and titanium dioxide nanoparticles elicit distinct apoptotic pathways in bronchial epithelial cells. Part Fibre Toxicol 7:10.

Hussain SM, Hess KL, Gearhart JM, Geiss KT, Schlager JJ. 2005. In vitro toxicity of nanoparticles in BRL 3A rat liver cells. Toxicol In Vitro 19:975–983.

IARC, International Agency for Research on Cancer. 2006. Monographs on the evaluation of carcinogenic risks to humans. Available from http://monographs.iarc.fr/ENG/,eetings/93-titaniumdioxide.pdf 93.

Johnston HJ, Hutchison GR, Christensen FM, Peters S, Hankin S, Stone V. 2009. Identification of the mechanisms that drive the toxicity of TiO(2) particulates: the contribution of physicochemical characteristics. Part Fibre Toxicol 6:1–33.

Kim IS, Baek M, Choi SJ. 2010. Comparative cytotoxicity of Al2O3, CeO2, TiO2 and ZnO nanoparticles to human lung cells. J Nanosci Nanotechnol 10:3453–3458.

Kumar A, Pandey A, Singh S, Shanker R, Dhawan A. 2011. Cellular uptake and mutagenic potential of metal oxide nanoparticles in bacterial cells. Chemosphere 83:1124–1132.

Liu S, Xu L, Zhang T, Ren GYang Z. 2010. Oxidative stress and apoptosis induced by nanosized titanium dioxide in PC12 cells. Toxicology 267:172–177.

Mosmann T. 1983. Rapid colorimetric assay for cellular growth and survival: application to proliferation and cytotoxicity assays. J Immunol Methods 65:55–63.

Park EJ, Yi JC, KH RD, Choi J, Park K. 2008. Oxidative stress and apoptosis induced by titanium dioxide nanoparticles in cultured BEAS-2B cells. Toxicol Lett 180:222–229.

Petkovic J, Zegura B, Stevanovic M, Drnovsek N, Uskokovic D, Novak S, et al. 2011. DNA damage and alterations in expression of DNA damage responsive genes induced by TiO(2) nanoparticles in human hepatoma HepG2 cells. Nanotoxicology 5(3):341–353.

Salvioli S, Ardizzoni A, Franceschi C, Cossarizza A. 1997. JC-1, but not DiOC6(3) or rhodamine 123, is a reliable fluorescent probe to assess delta psi changes in intact cells: implications for studies on mitochondrial functionality during apoptosis. FEBS LETT 411:77–82.

Sharma V, Shukla RK, Saxena N, Parmar D, Das M, Dhawan A. 2009. DNA damaging potential of zinc oxide nanoparticles in human epidermal cells. Toxicol Lett 185:211–218.

Sharma V, Singh SK, Anderson D, Tobin DJ, Dhawan A. 2011. Zinc Oxide nanoparticle induced genotoxicity in primary human epidermal keratinocytes. J Nanosci Nanotechnol 11:3782–3788.

Shukla RK, Kumar A, Pandey AK, Singh SS, Dhawan A. 2011a. Titanium dioxide nanoparticles induce oxidative stress-mediated apoptosis in human keratinocyte cells. J Biomed Nanotechnol 7:100–101.

Shukla RK, Sharma V, Pandey AK, Singh S, Sultana S, Dhawan A. 2011b. ROS-mediated genotoxicity induced by titanium dioxide nanoparticles in human epidermal cells. Toxicol In Vitro 25:231–241.

Singh NP, McCoy MT, Tice RR, Schneider EL. 1988. A simple technique for quantitation of low levels of DNA damage in individual cells. Exp Cell Res 175:184–191.

Song YS, Lee BY, Hwang ES. 2005. Dinstinct ROS and biochemical profiles in cells undergoing DNA damage-induced senescence and apoptosis. Mech Ageing Dev 126:580–590.

Suzuki H, Toyooka T, Ibuki Y. 2007. Simple and easy method to evaluate uptake potential of nanoparticles in mammalian cells using a flow cytometric light scatter analysis. Environ Sci Technol 41:3018–3024.

Tice RR, Agurell E, Anderson D, Burlinson B, Hartmann A, Kobayashi H, et al. 2000. Single cell gel/comet assay: guidelines for in vitro and in vivo genetic toxicology testing. Environ Mol Mutagen 35:206–221.

Trouiller B, Reliene R, Westbrook A, Solaimani P, Schiestl RH. 2009. Titanium dioxide nanoparticles induce DNA damage and genetic instability in vivo in mice. Cancer Res 69:8784–8789.

Valko M, Izakovic M, Mazur M, Rhodes CJ, Telser J. 2004. Role of oxygen radicals in DNA damage and cancer incidence. Mol Cell Biochem 266:37–56.

Wan CP, Myung E, Lau BH. 1993. An automated micro-fluorometric assay for monitoring oxidative burst activity of phagocytes. J Immunol Methods 159:131–138.

Wang J, Zhou G, Chen C, Yu H, Wang T, Ma Y, et al. 2007a. Acute toxicity and biodistribution of different sized titanium dioxide particles in mice after oral administration. Toxicol Lett 168:176–185.

Wang JJ, Sanderson BJ, Wang H. 2007b. Cyto- and genotoxicity of ultrafine TiO2 particles in cultured human lymphoblastoid cells. Mutat Res 628:99–106.

Xia T, Kovochich M, Liong M, Dler LM, Gilbert B, Shi H, et al. 2009. Comparison of the mechanism of toxicity of zinc oxide and cerium

oxide nanoparticles based on dissolution and oxidative stress properties. ACS Nano 2(10):2121–2134.
Xu A, Chai Y, Nohmi T, Hei TK. 2009. Genotoxic responses to titanium dioxide nanoparticles and fullerene in gpt delta transgenic MEF cells. Part Fibre Toxicol 6:3.
Zhao J, Bowman L, Zhang X, Vallyathan V, Young SH, Castranova V, et al. 2009. Titanium dioxide (TiO2) nanoparticles induce JB6 cell apoptosis through activation of the caspase-8/Bid and mitochondrial pathways. J Toxicol Environ Health A 72:1141–1149.